

# Seismic Anisotropy of Mafic Blueschists: Constraints from Exhumed Rock-Record with Implications for the Subduction Interface

Jason N. Ott<sup>1</sup>, Cailey B. Condit<sup>1</sup>, Rachel Bernard<sup>2</sup>, Vera Schulte-Pelkum<sup>3</sup>, and Matej Pec<sup>4</sup>

<sup>1</sup>Department of Earth and Space Sciences, University of Washington, Seattle WA <sup>2</sup>Geology Department, Amherst College, Amherst MA  
<sup>3</sup>Cooperative Institute for Research in Environmental Sciences and Department of Geological Sciences, University of Colorado, Boulder CO  
<sup>4</sup>Department of Earth, Atmospheric and Planetary Sciences, Massachusetts Institute of Technology, Cambridge MA



## I. Motivation

- Loading of seismogenic zone and production of arc-magmas driven by ductile deformation and metamorphic reactions at plate interface
- Seismic anisotropy can illuminate subduction zone structure and link deep processes to geological hazards at the surface
- Constraining the seismic anisotropy of mafic blueschists, a key constituent of subducting slabs, will improve imaging of the subduction zone interface

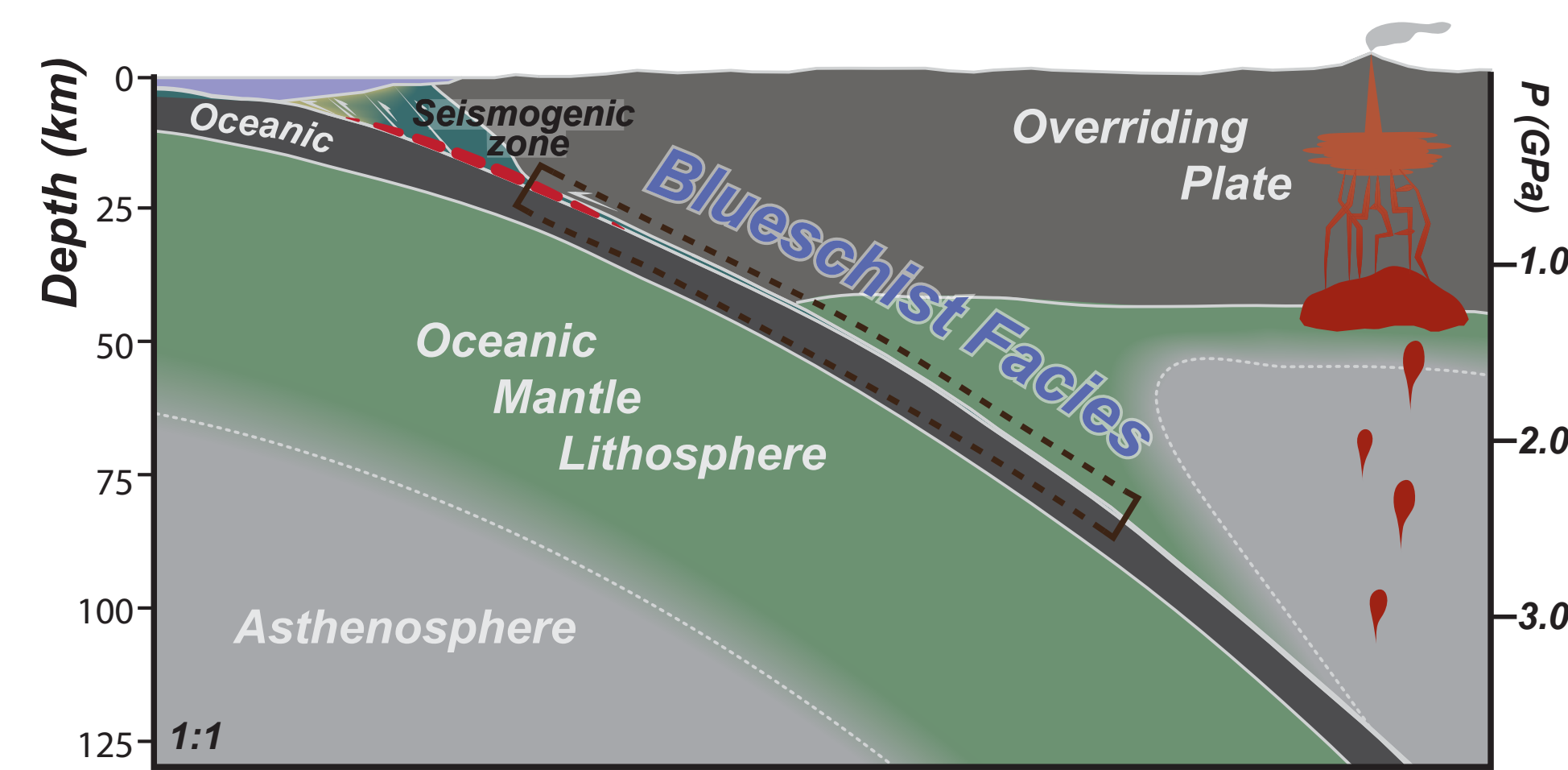
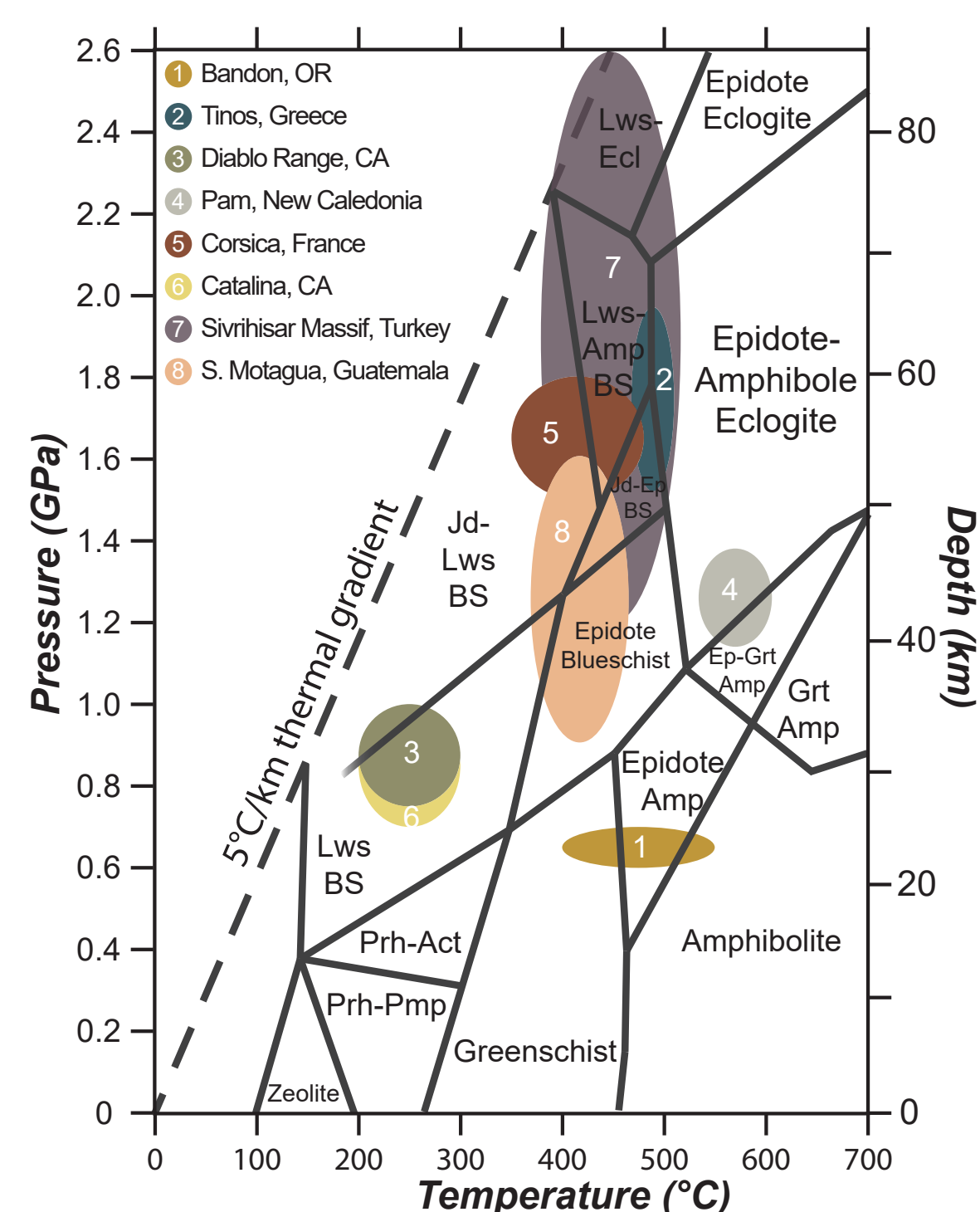


Diagram of a typical subduction zone illustrating major structural features and increasing pressure with depth

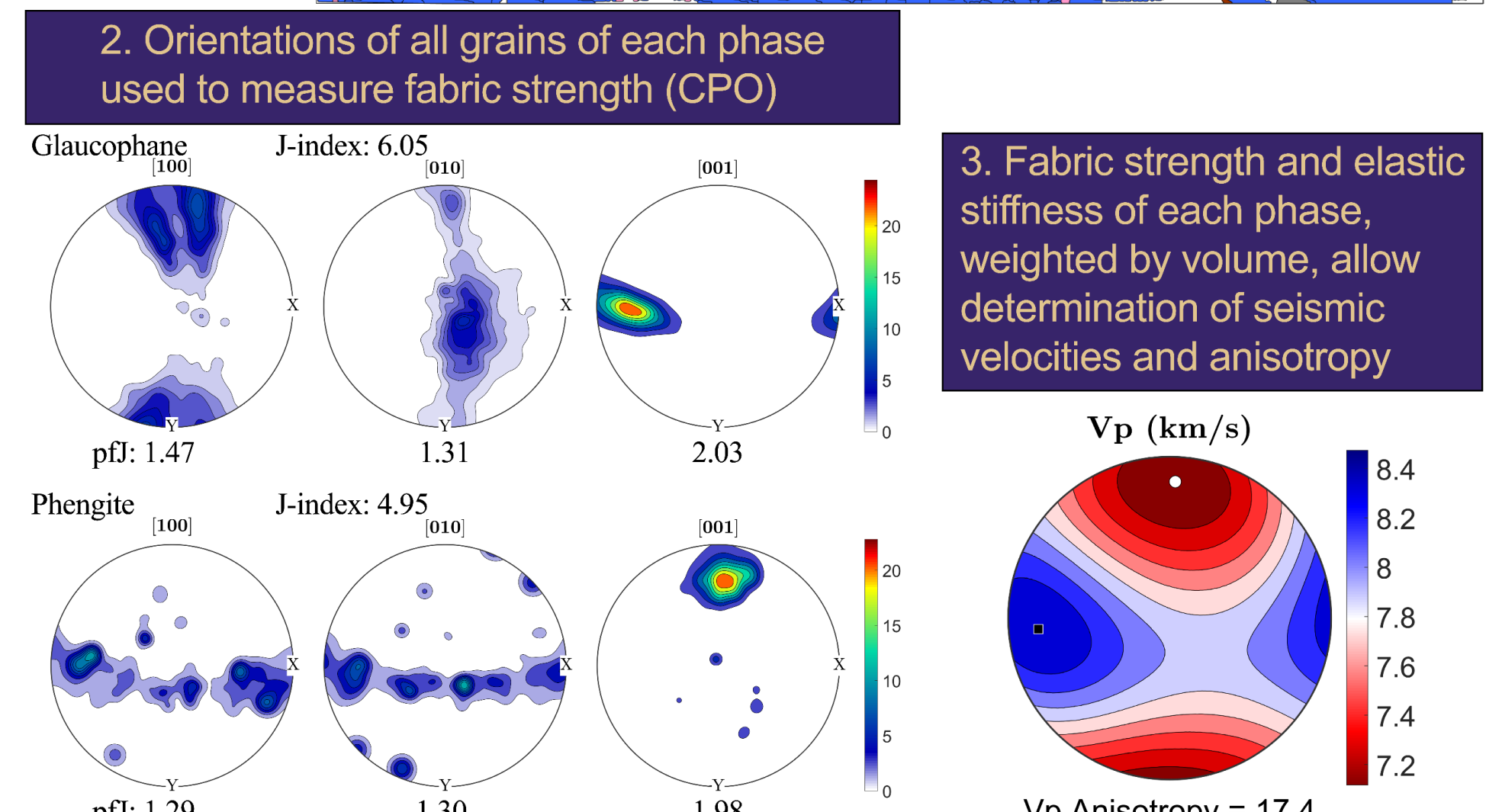
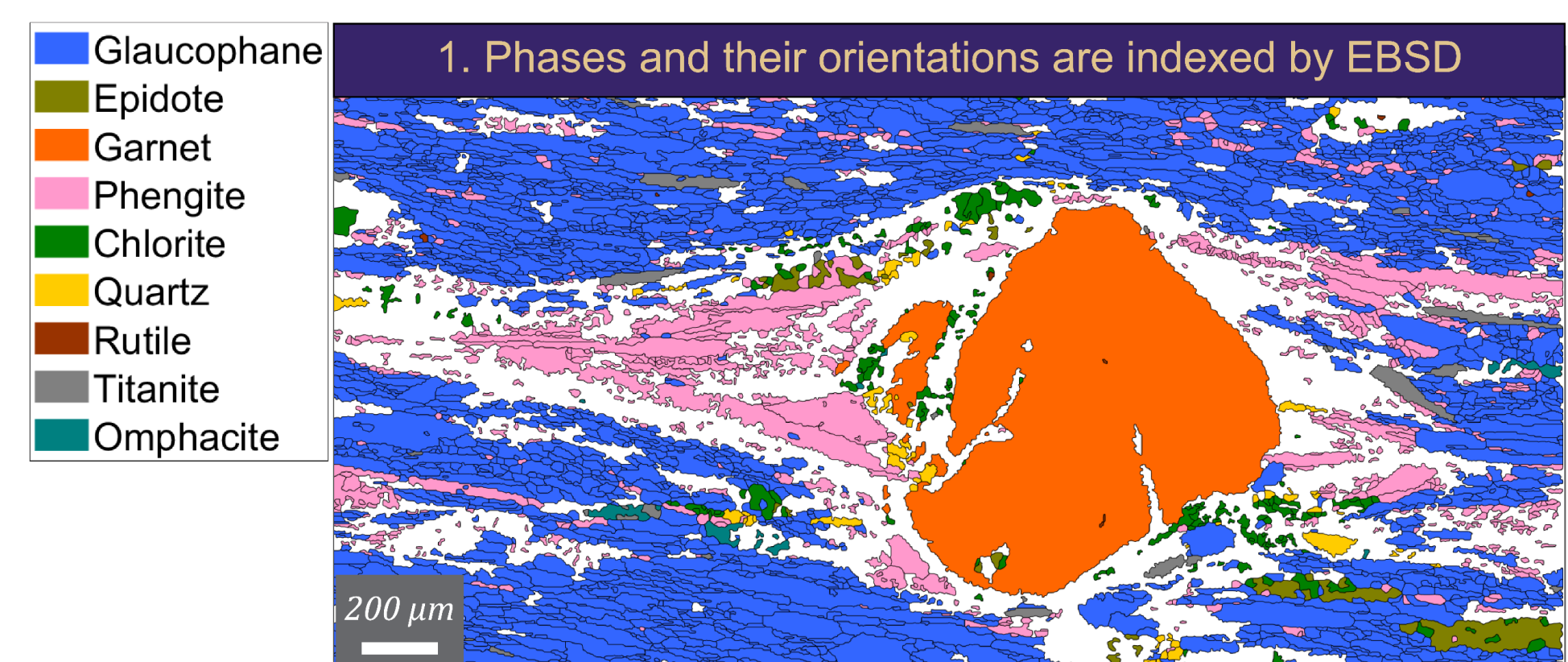
## II. Materials

- 14 mafic blueschists from 8 exhumed subduction terranes
- 9 epidote blueschists
- 5 lawsonite blueschists
- Variable mineralogies spanning a broad range of the blueschist facies P-T conditions
- Samples display diverse deformation histories preserved as lineation, foliation, and crystallographic preferred orientation (CPO)
- Samples prepared thin sections prepared (foliation normal/lineation parallel) for EBSD analysis



Blueschist sample P-T estimates from the literature overlain on metamorphic facies diagram (after Peacock, 2009)

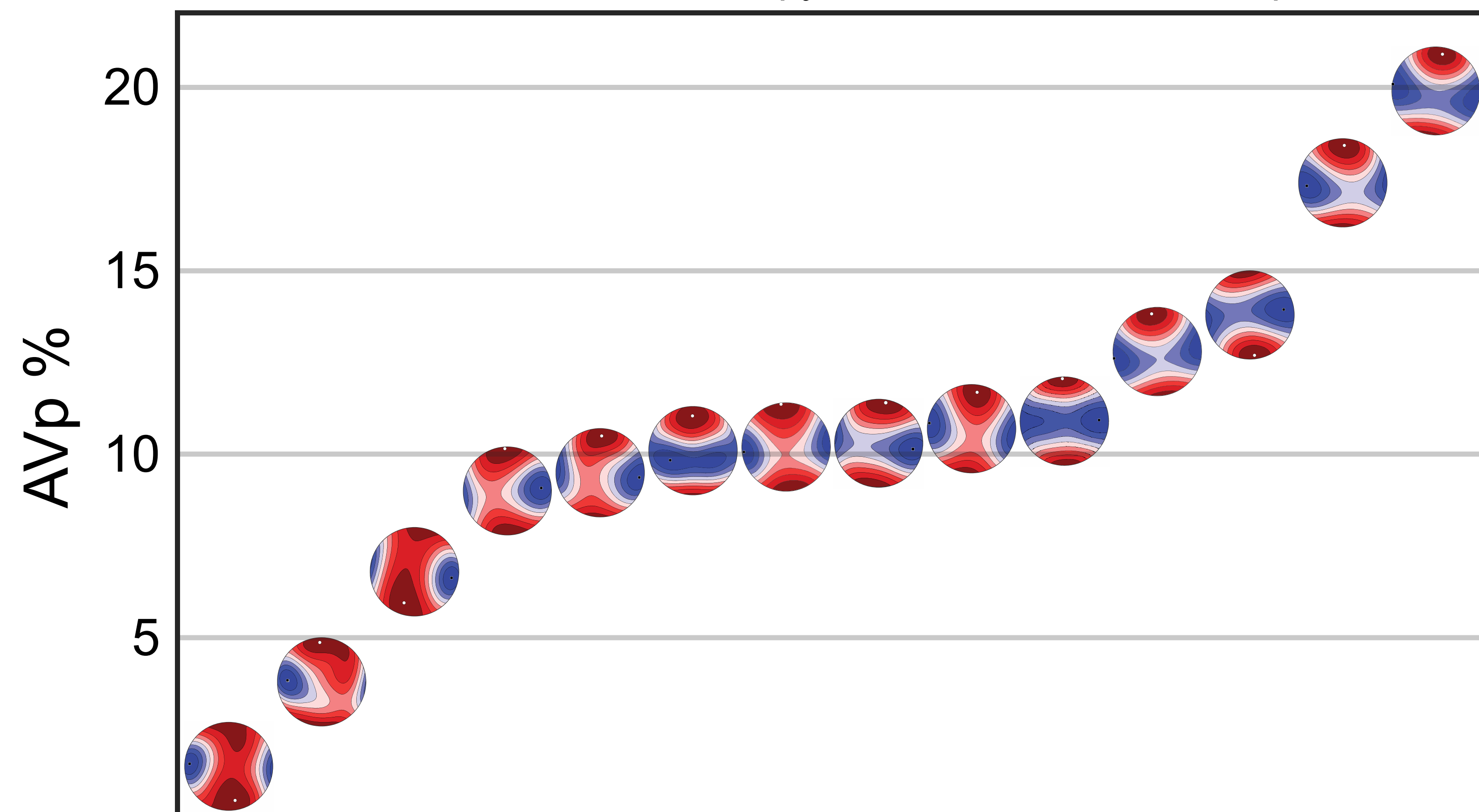
## III. Methods



Blueschists show strong seismic anisotropy (up to 20%), scaling with glaucophane abundance & fabric strength. This suggests potential for improved imaging of subducting slabs with receiver functions.

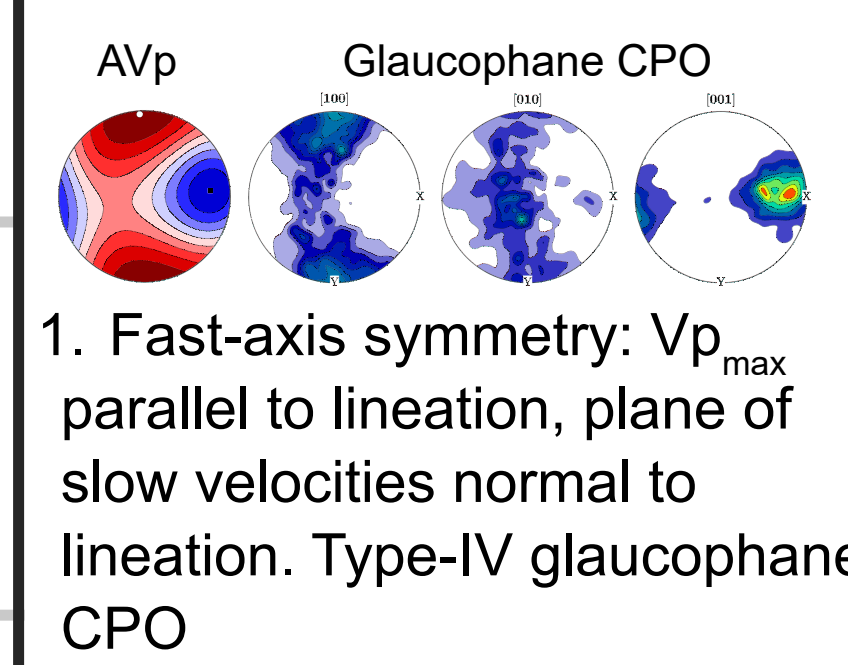
## IV. Results and Discussion

### P-Wave Seismic Anisotropy of Mafic Blueschist Samples



### AVp Symmetry

Seismic velocity patterns show 2 symmetry types

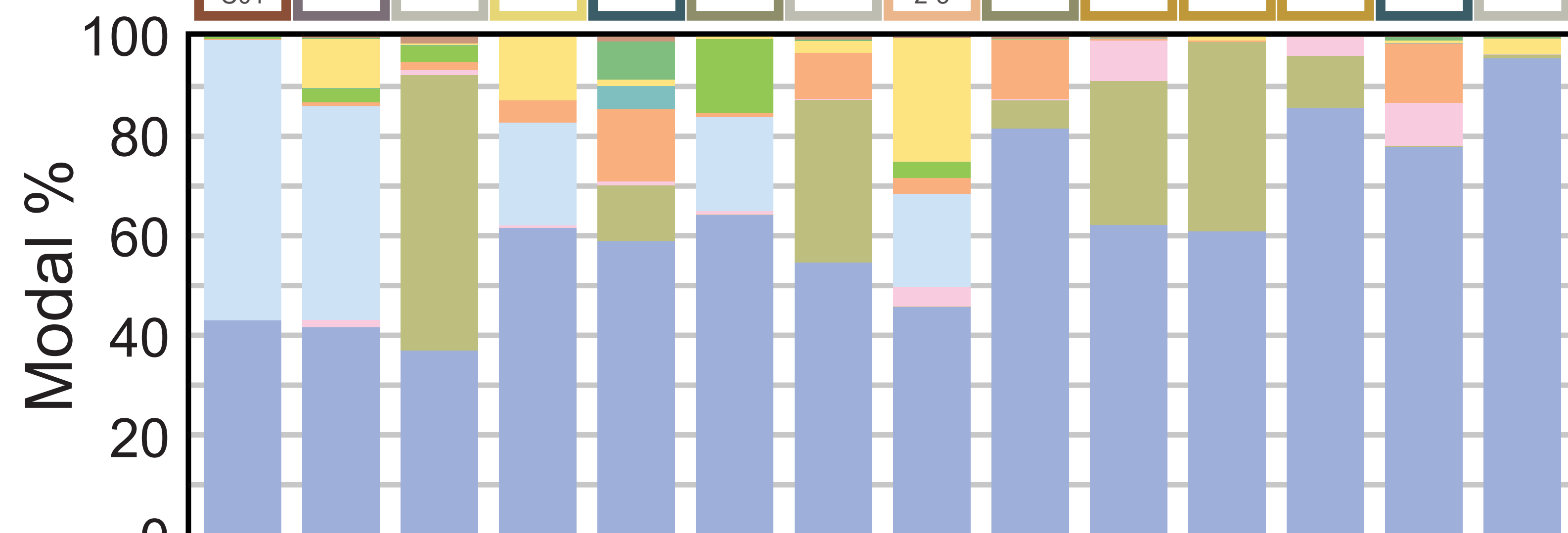


1. Fast-axis symmetry:  $V_{p,max}$  parallel to lineation, plane of slow velocities normal to lineation. Type-IV glaucophane CPO

2. Slow-axis symmetry:  $V_{p,min}$  normal to foliation, fast velocities in foliation plane. Type-I glaucophane CPO

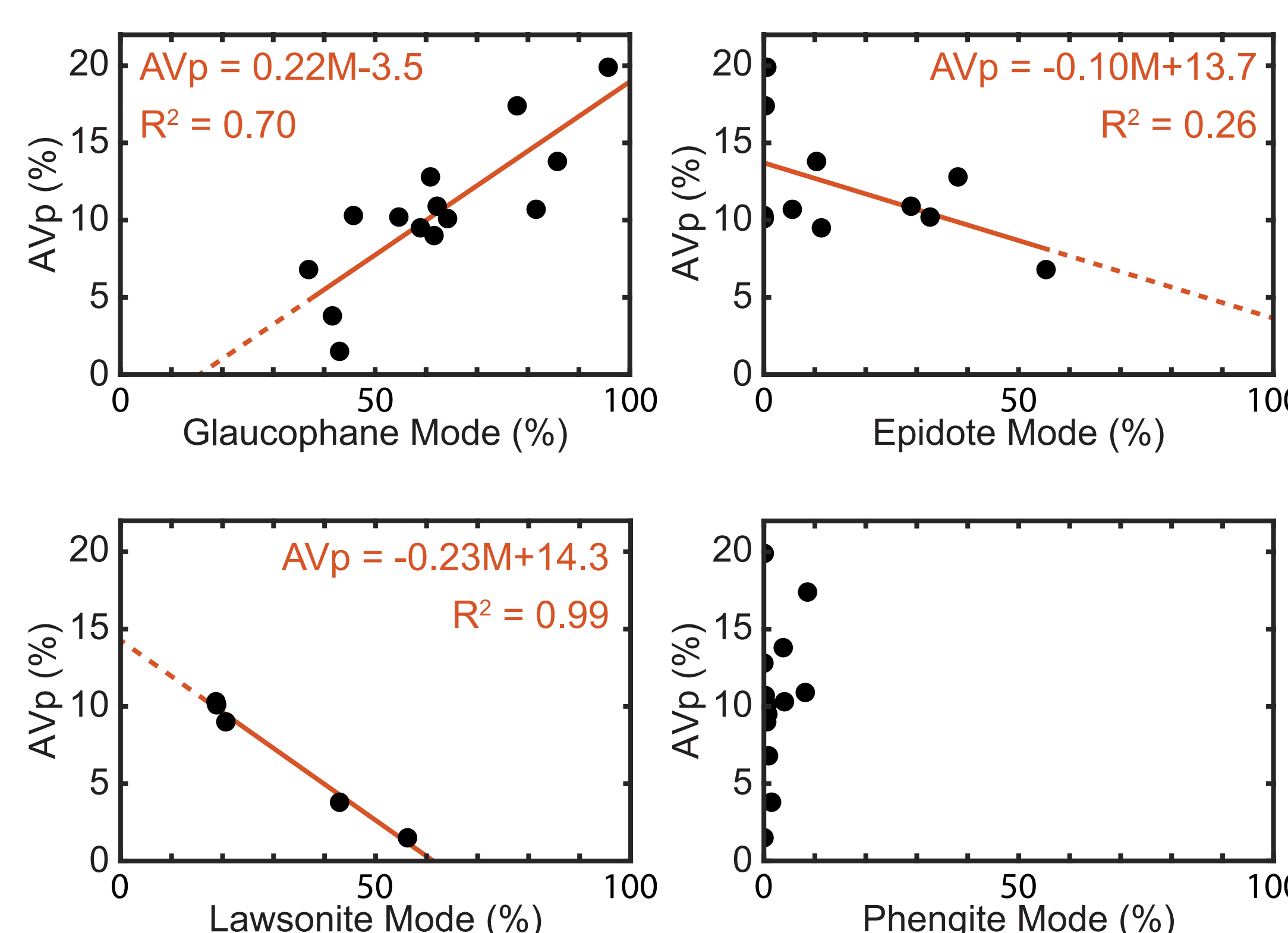
### Minerals

- Glaucophane
- Epidote
- Lawsonite
- Quartz
- Phengite
- Garnet
- Omphacite
- Jadeite
- Chlorite
- Rutile
- Titanite



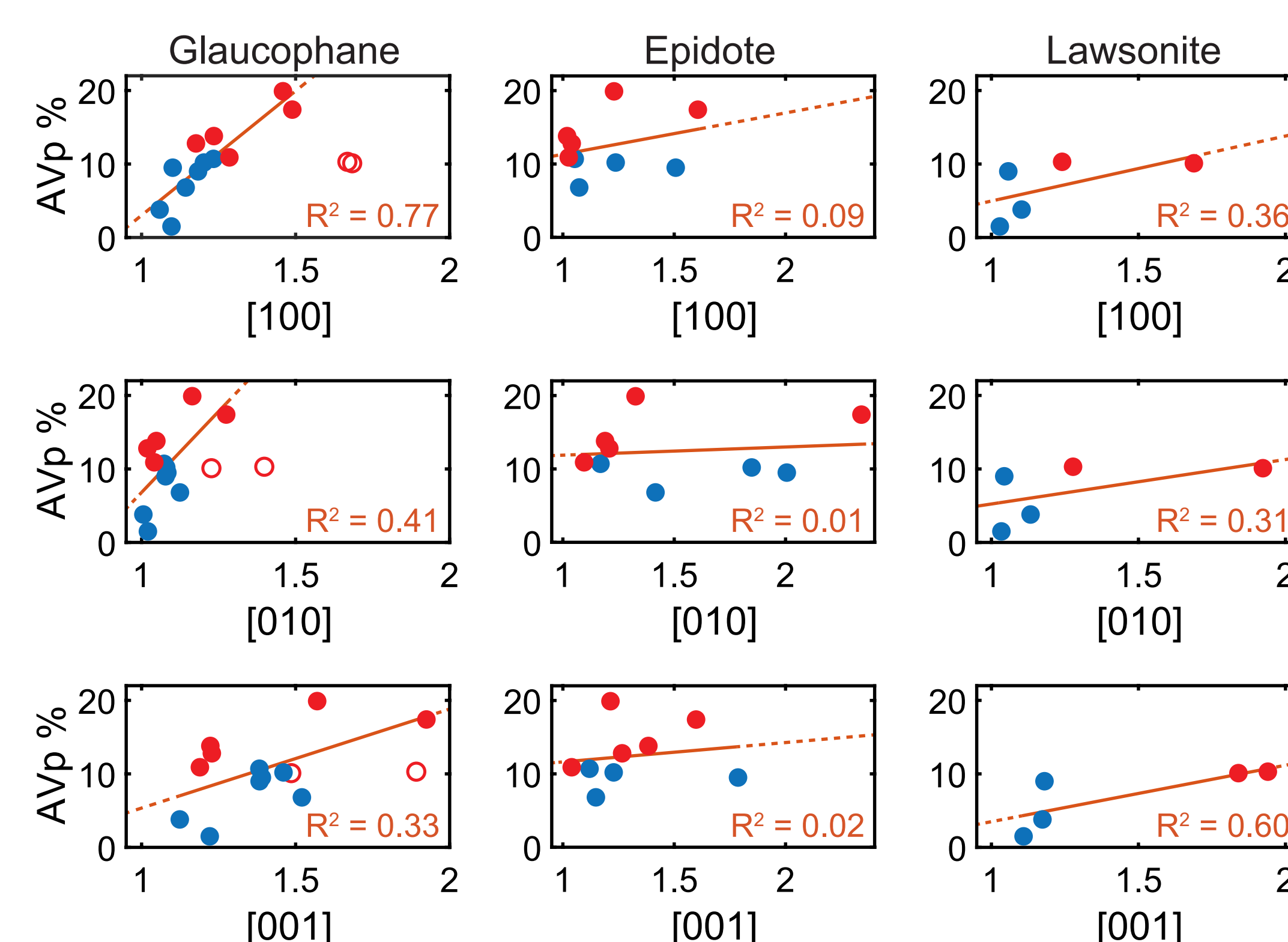
Top: Seismic anisotropy in  $V_p$  (AVp %) of samples in order of increasing anisotropy. Samples with fast-axis symmetry display AVp up to ~10%, slow-axis symmetry for samples with AVp ~10-20%. Bottom: sample composition in order of increasing anisotropy. Samples ~80% or greater highly anisotropic phases

### AVp % versus Modal Abundance



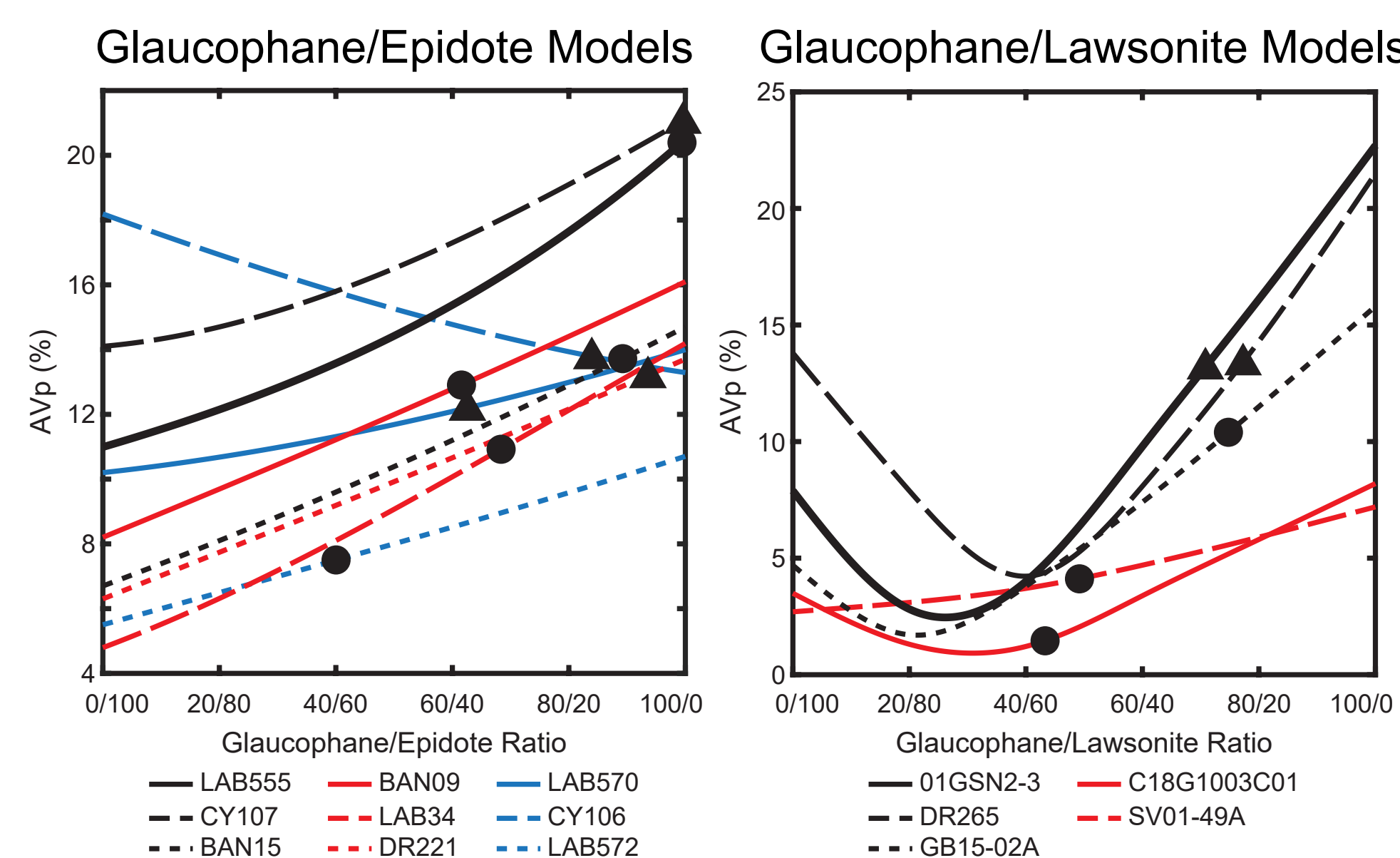
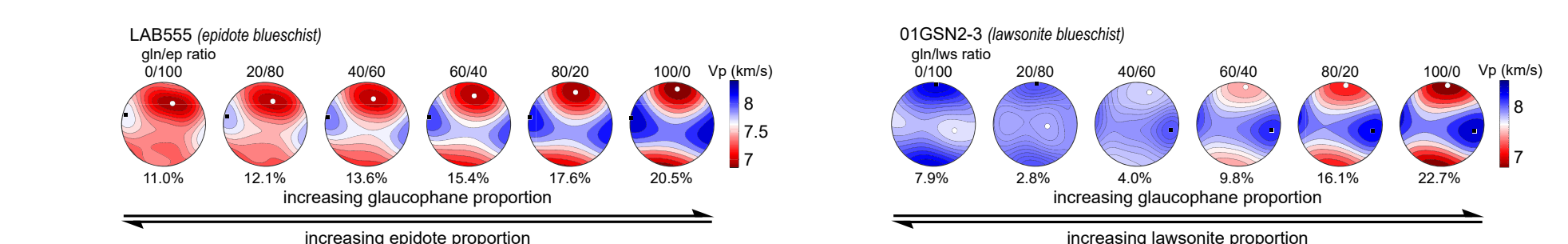
Seismic anisotropy versus modal abundance of glaucophane, epidote, lawsonite, and phengite. AVp % increases with increasing glaucophane abundance, but is diluted by increasing fractions of epidote or lawsonite. No AVp trend with increasing phengite

### AVp % versus Fabric Strength (pJ-Index)



AVp % vs CPO for each crystallographic axis (measured as pJ-Index) for glaucophane, epidote, and lawsonite. AVp shows strongest increase with CPO in glaucophane [100] and [010] axes, only weakly increases with epidote and lawsonite fabric strength

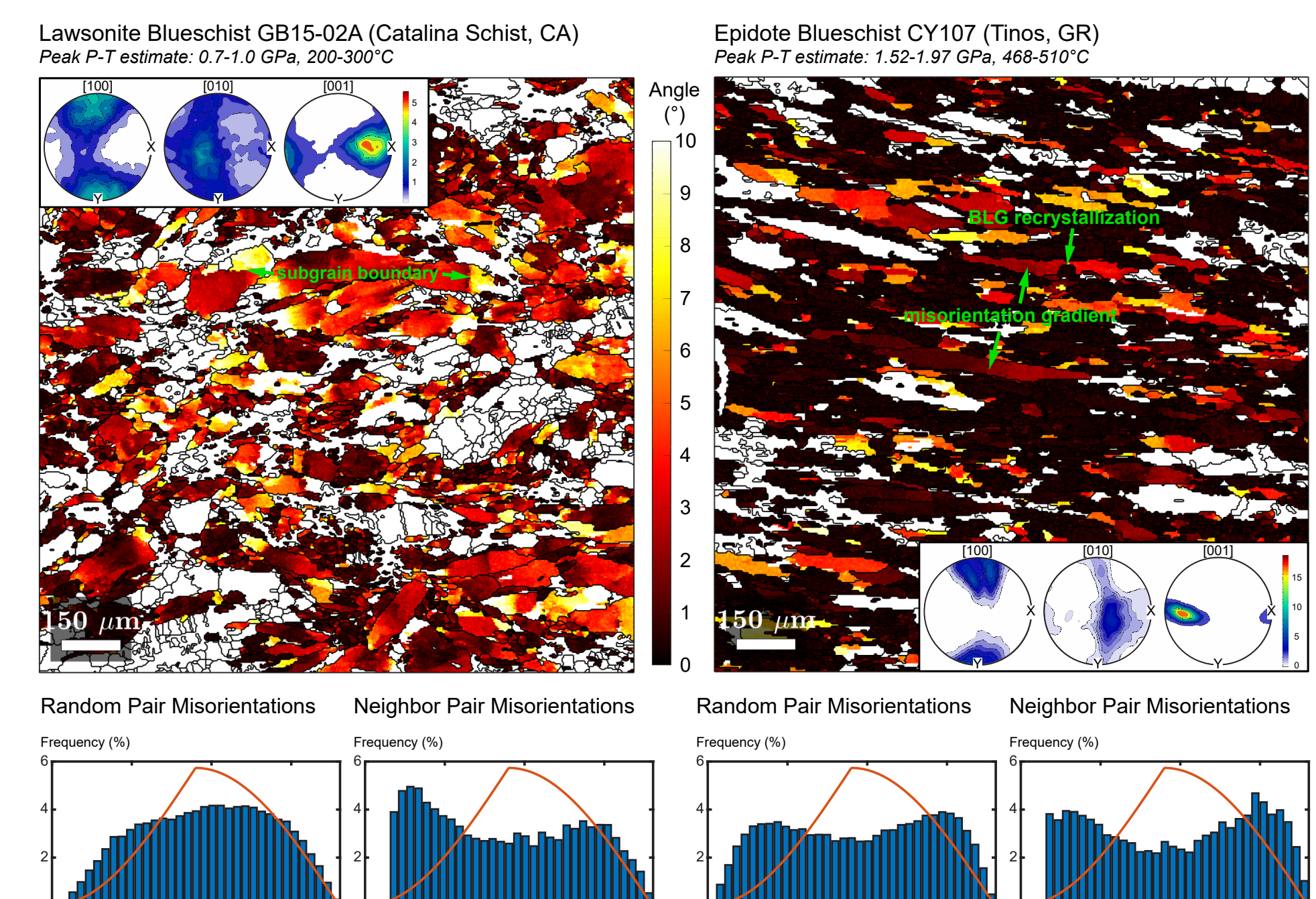
## Rock-Recipe Modeling



AVp for gln/ep 2-phase models show monotonic increase with glaucophane abundance.  $V_{p,max/min}$  consistently oriented due to complementary CPOs in glaucophane and epidote

AVp for gln/lws 2-phase models show concave profile with min ~20-40% glaucophane. Symmetry of anisotropy ( $V_{p,max/min}$  direction) changes at min due to antithetical gln/lws CPOs

## Glaucophane Deformation Microstructures



Misorientation to mean orientation maps (top L, R) show misorientation gradients, subgrain boundaries, and bulging recrystallization structures. Misorientation distributions (bottom) differ from untextured distribution (red curve), with higher frequency of low angle boundaries in neighboring grain-pairs (subgrain boundary recrystallization). The microstructural evidence is consistent with CPO-formation by climb-accommodated dislocation creep throughout blueschist stability field

## V. Key Takeaways

- Mafic blueschists display a broad range of p-wave seismic anisotropy, ranging from AVp = 6.8 - 19.9% in epidote blueschists and AVp = 1.5 - 10.3% in lawsonite blueschists.
- Blueschist anisotropy is largely governed by glaucophane, increasing with both glaucophane modal abundance and CPO-strength.
- Increasing epidote/lawsonite dilutes bulk anisotropy; this effect is most pronounced in lawsonite due to antithetical fast/slow  $V_p$ -directions in lawsonite CPO versus glaucophane CPO.
- Blueschist anisotropy develops largely from ductile deformation and CPO formation in glaucophane by dislocation creep, active in glaucophane throughout blueschist stability field.

## VI. References



**Acknowledgements:** Funding for this work is provided by the National Science Foundation Division of Earth Science (NSF EAR-XXXXXX). Part of this work was conducted at the Molecular Analysis Facility, which is supported in part by funds from the Molecular Engineering & Sciences Institute, the Clean Energy Institute, the National Science Foundation (NNCI-2025489 and NNCI-1542101). The authors are indebted to Darrel S Cowan, Donna Whitney, Kayleigh Harvey, and Joshua M Garber for samples provided for inclusion in this study.